Journal of Ovonic Research Vol. 12, No. 3, May - June 2016, p. 171 - 184

EFFECT OF GROWTH TIME ON STRUCTURE, OPTICAL AND PHOTO-RESPONSE CHARACTERISTICS OF ZnO NANORODS DEPOSITED ONTO VARIOUS SUBSTRATES

R. A. TALIB[a,b*], M. J. ABDULLAH[a], H. S. AL-SALMAN[c],
S. M. MOHAMMAD[a], N. M. AHMED[a], M. BOUOUDINA[d]
[a]*Nano-Optoelectronics Research and Technology (NOR), School of Physics, UniversitiSains Malaysia, 11800 Penang, Malaysia*
[b]*Polymer Research Center, University of Basra, Iraq*
[c]*Department of Physics, College of Science, University of Basrah, Basrah, Iraq*
[d]*Department of Physics, College of Science, University of Bahrain, PO Box 32038, Kingdom of Bahrain*

ZnO nanorod (NRs) were deposited by chemical bath deposition at different growth duration time onto a variety of substrates (glass, polyethylene terephthalate (PET), n-type Si, and stainless steel). X-ray diffraction analysis confirms that all grown films crystallize within the hexagonal wurtzite-type structure with a strong preferred orientation along (002) for Si-substrate. Scanning electron microscopy observations reveal the formation of nanorods, where both density and length increase with the increase of deposition time. The optical band gap determined from PL spectra was found of ZnO (NRs) grown onto Si substrate at 2 and 3h is close to the value of the energy gap of bulk ZnO (E_g=3.37 eV), which can be associated with the low defects level. Raman spectroscopy analysis revealed the presence of a compressive stress within ZnO nanorods for all substrates. Metal-semiconductor-metal device was fabricated and UV photo-responsivity at room temperature was studied as function of the nature of substrate. The results showed that the UV photo-detector based on ZnO nanorods deposited (3h) onto n-Si showed a high sensitivity of 6250% at zero bias voltage.

(Received April 21, 2016; Accepted June 30, 2016)

*Keywords :*ZnO; substrate nature; chemical bath deposition; PL.

1. Introduction

In recent years, many research works have been devoted on ZnO based nanostructures due to their interesting and unique properties, which offer various applications including gas sensors [1, 2], solar cells [3, 4], light emitting diodes (LEDs) [5], etc. ZnO nanostructures have been prepared by different physical, chemical, and electro chemical methods. However, chemical methods have attracted particular interest because of their numerous advantages including possibility of controlling the shape and size of the particles/grains by setting different growth parameters, low cost and environmental friendly [6, 7]. ZnO with its relatively high melting point 2251 K [8], crystallizes within a hexagonal wurtzite-type crystal structure having lattice constants a=0.325 nm, c= 0.521 nm [9].

It is important to highlight that in order to use of ZnO nanostructures as UV detector, two conditions must be taken into consideration: (i) firstly, the film characteristics are substrate-nature dependent in addition to the deposition method; and (ii) secondly, the metal-semiconductor contact plays a key role during device. Ohmic or Schottky contact forms depending on the semiconductor (Φ_s) and metal work (Φ_m) function.

ZnO nano structured films are regarded as one of the most promising candidate for the development of high quality and cost-effective UV photodetector with high performances. The UV

Corresponding author: rounq4@gmail.com

photoresponse in ZnO films was firstly observed by Mollow in the 1940s [10]. However, the research devoted to ZnO-based photoconductivity thrived gradually since the 1980s[11]; the fabricated devices usually have simple structure and the observed properties are not really very good.

In this paper, the effects of different deposition time (2 and 3 h) and various substrates (glass, PET, Si and stainless steel) on the growth of ZnO films, were investigated. The chemical bath deposition (CBD) was adopted. The UV photo-response of the as-fabricated metal-semiconductor-metal (MSM) Schottky contact onto ZnO nanrods based film was analysed.

2. Experimental Part

2.1 Growth of ZnOnanorods onto substrates

ZnO nanostructures were synthesized using a low temperature aqueous solution growth method. The substrates were properly cleaned prior to deposition. Glass, PET and stainless steel substrates were cut into small pieces and ultrasonically cleaned then dried using dry nitrogen (N_2) flow.

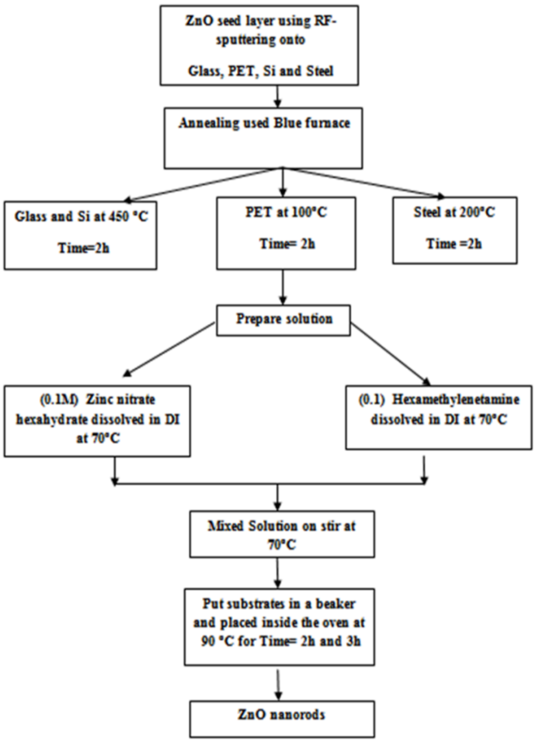

Fig. 1: Scheme for ZnO(NRs) deposition using chemical bath deposition process.

The n-type Si-wafers were cut using diamond cutting machine and subsequently cleaned following the Radio Corporation of America (RCA) method [12]. A ZnO buffer layer of 130 nm thickness was coated onto all substrates by radio frequency (RF) sputtering, using high-purity Ar gas as plasma to sputter the target, a chamber pressure of $1.82*10^{-2}$ mbar and an RF power of 150 W. For the growth solution, 0.1 mol/L zinc nitrate hexahydrate [$Zn(NO_3)_2.6H_2O$] 0.1 mol/L hexamethylenetelramine ($C_6H_{12}N_4$) were dissolved separately in de-ionized (DI) water at 70°C, then both solutions were mixed in a beaker containing beforehand the ZnO seeded substrate and after that placed inside an oven for a certain period of time (2 and 3h) at 90°C[13]. Finally, the as obtained films were washed with deionizer (DI) water and hot ethanol. Figure (1) shows the scheme for ZnO films preparation using CBD method.

2.2 Characterizations

The morphology of ZnO nanorods films was investigated by field emission scanning electron microscopy (FESEM) using FEI Nova Nano SEM 450. The structure was checked by high-resolution X-ray diffraction (HR-XRD) using PANalyticalX'Pert Pro MRD system equipped with Cu-Kα radiation source (λ=0.1541 nm) operating at 40 kV and 20 mA. The XRD patterns were recorded in the 2θ range of 20^o-70^o. The optical properties were studied at room temperature using a Shimadzu UV–Vis 1,800 spectrophotometer. Raman spectroscopy spectra were recorded at room temperature using JobinYvon HR 800 UV (Edison, USA). A current source 2400 source Meter, Keithely (Cleveland Ohio, USA) was used to measure the electrical characteristics of the UV-sensing devices.

2.3 Photodetector Fabrication

The fabrication of UV photodetector involved the deposition of platinum (Pt) electrodes onto the surface of ZnO(NRs) arrays onto the glass, PET, Si and steel substrates (Figure 2). The Pt electrodes were deposited using a 200 nm thick suitable mask via the RF-sputtering model Edwarda A500 at room temperature. After evacuating the chamber to $2x10^{-5}$ mbar, the RF-power of the high purity target (99.99%) was maintained at 150W.

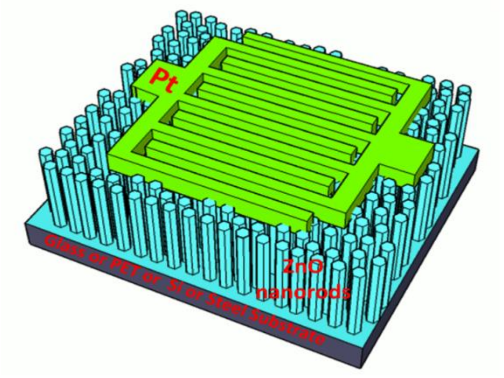

Fig. 2: Schematic illustration of the ZnO(NRs) on various substrate UV device.

3. Result and Discussion

3.1 Morphological Observations

FESEM images of the as-deposited ZnO films are given in Figure(3). It can be seen that hexagonally-shaped ZnO nanorods (NRs) were grown vertically(perpendicular to the substrate surface). It can be noticed also that the density and length of ZnO NRs increase towards c-axis orientation when increasing growth time from 2h (Fig.3(a)) to 3h (Fig. 3(b)). This can explained as follow: when increasing the deposition time, the number of ion hydroxide (OH^-) and ion zinc (Zn^{+2}), comes from disintegration of hexamethylenetetramine and zinc nitrate hexahydrate increase and attracted toward the c-axis direction [14]. For all films, the diameter of the formed NRs ranges up to about 50nm. The inset in Fig. 3 shows that the length of NRs has changed drastically from 588nm to 910nm, for a deposition time of 2 and 3 h, respectively. Also, it can be seen from figure 3 that the NRs are more vertically aligned with high density when using Si substrate, followed by stainless steel substrate.

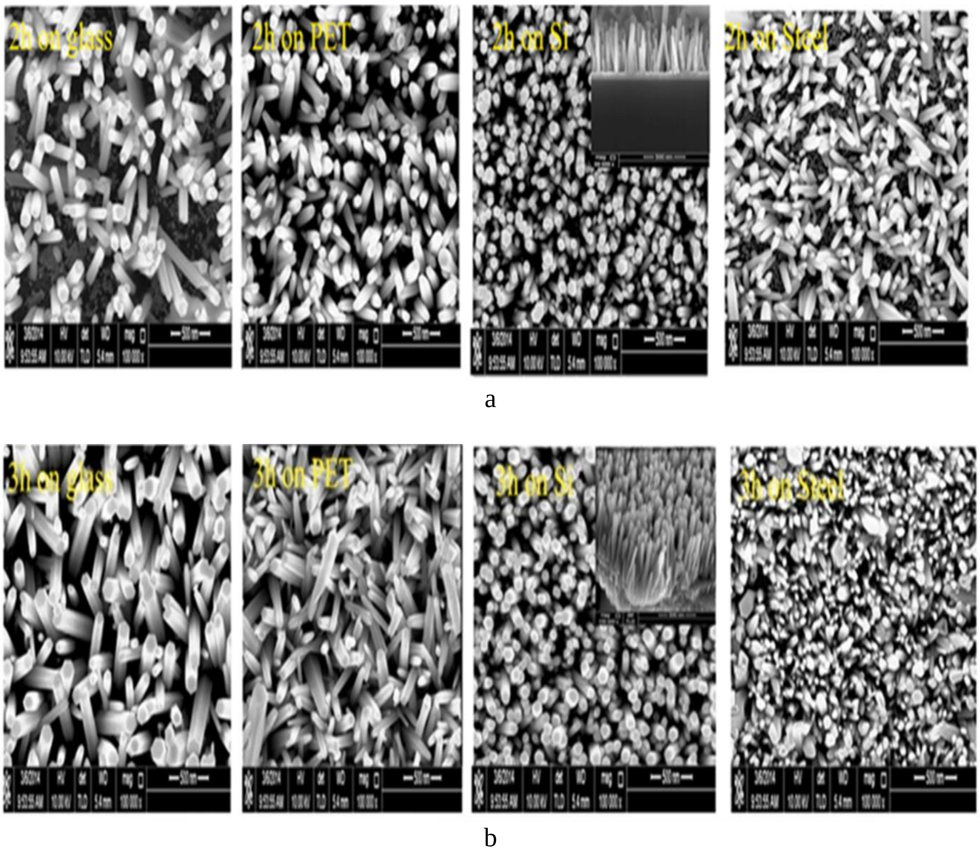

Fig. 3: FESEM images of ZnO NRs deposited at (a) 2h and (b) 3h onto various substrates.

3.2 X-ray Diffraction Analysis

X-ray diffraction (XRD) patterns of the as-deposited ZnO films are reported in Figure4. All the observed peaks originate from the hexagonal wurtzite-type ZnO crystal structure [15]. The strong and sharp diffraction peaks indicate a high crystallinity. The XRD patterns of for a deposition time of 2h (Figure 4a) show a strong (002) peak and weak (100) (101) and (103) peaks. Similar behaviour is observed for the films deposited for 3 h (Figure 4b), but the intensity of (002) peak is more pronounced. This implies that the as-grown NRs have perfect c-axis preferred orientation which is in accordance with FESEM observations. It can be also noticed that the (002) reflection intensity for ZnO deposited onto Si substrate is higher followed by stainless steel substrate, which indicates good quality and crystallinty of ZnO NRs, and once again in agreement with FESEM observations. The peaks located at 69.2^o was attributed to Si originated from Si-substrate while the peaks located at 25.97^{o}originated from PET substrate and the peaks located at 43^o, and 51^o from Steel substrate.

The lattice constant *c* and strain along c-axis ($\mathcal{E}_{zz}$) of ZnO wurtize can be calculated by using the following relations, respectively[7, 16]:

$$C = \frac{\lambda}{\sin\theta} \qquad (1)$$

$$e_{ZZ} = \frac{C - C_o}{C_o} \text{x}100\% \qquad (2)$$

where λ=0.15405 nm is the wavelength of the X-ray source, θ is the angle of the diffraction peak and C_o the standard lattice constant for unstrained ZnO (0.5215 nm according to JCPDS card No. 80-0075). The results are reported in Table 1. It can be noticed that all structural (lattice constant

c) and micro structural (strain $\mathcal{E}_{zz}$) parameters are sensitive to the type of substrate and the deposition time. The negative value of strain for ZnO NRs is related to the compressive strain [17]. This may be attributed to the mismatch existing between the lattice parameter of ZnO film (a= 3.2539 nm and c= 5.2098 nm) and the lattice paremeters of the substrates used in this study at 3h (a_{glass}= 3.0051 nm$_{l}$; a_{PET}= 3.0067 nm; a_{Si}= 3.0060; $a_{stainlessstee}$= 3.0073).

Table 1: Structural and microstructural characteristics of ZnO NRs grown onto different substrate for 2 h and 3 h.

Synthesized and deposited for 2 hours				**Synthesized and deposited for 3 hours**			
Substrate	**2θ (°) of (002)**	**c (Å)**	**ε_{zz}(%)**	**Substrate**	**2θ (°) of (002)**	**c (Å)**	**ε_{zz}(%)**
Glass	34.42	5.211	-0.0007	**Glass**	34.43	5.209	-0.0010
PET	34.48	5.201	-0.0026	**PET**	34.41	5.212	-0.0005
Si	34.42	5.211	-0.0007	**Si**	34.42	5.210	-0.0007
Stainless Steel	34.41	5.212	-0.0005	**Stainless Steel**	34.40	5.213	-0.0003

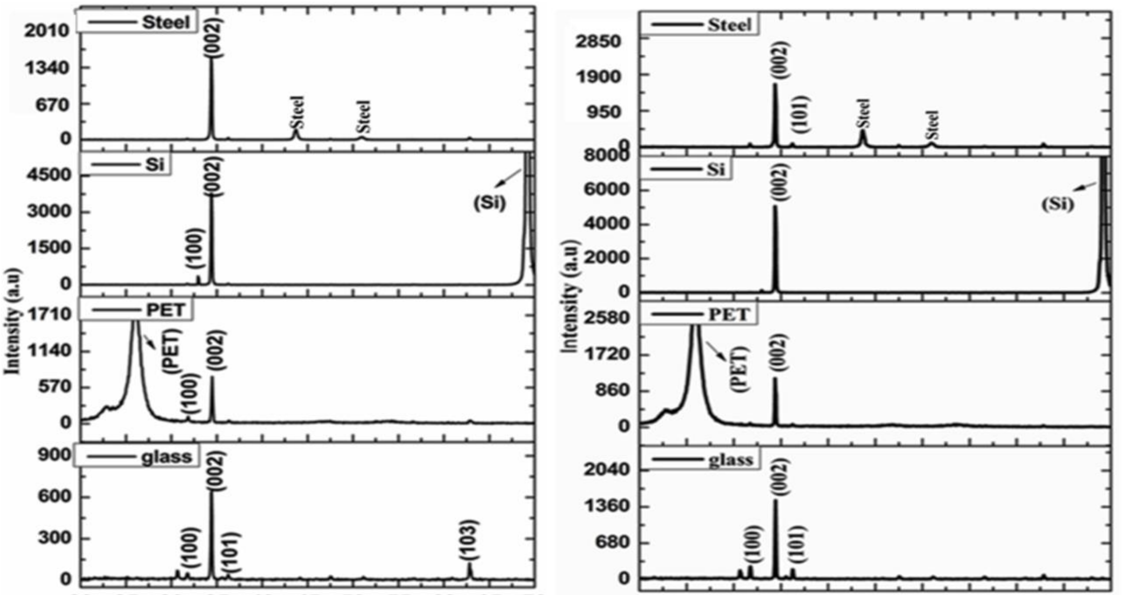

(a) (b)

Fig. 4: XRD patterns of ZnO NRs deposited at(a) 2h and (b) 3h onto various substrates.

3.3 Photoluminescence (PL) Characterization

Fig. 5(a and b) shows the PL spectra of ZnO (NRs) grown onto glass, PET, Si and Steel substrates at duration time 2h and 3h. All ZnO(NRs) films show a high emission peak at the ultraviolet (UV) region and a broad deep-level emission peak around the green emission. The ZnO (NRs) grown onto Si substrate show the highest UV intensity at duration time 3h with a lowest green emission, whereas the other samples showed a high UV intensity and different green emission intensity. This result is a good agreement with XRD and FESEM results. a high intensity emission at the ultraviolet with a low green emission, that is mean a good crystal quality of ZnO(NRs) [18, 19]. Thus, the ZnO grown onto Si and PET showed the best crystallization at duration time of 3h compared to 2h. For the UV emission, the peak wavelength is around 380nm while for green emission, the peak is around 537nm. The green emission peak is due to defects, such as impurities, Zn interstitials, and oxygen vacancies[19]. The summarized data for UV peak position and the corresponding energy gap as-obtained from PL spectra are reported in Table2. It can be observed that the energy gap of ZnO (NRs) grown onto Si substrate at 2 and 3h is close to the value of the energy gap of bulk ZnO (E_g=3.37 eV), which can be associated with the low defects level. For the remaining films, the values of band gap are found smaller, which is may be due to the presence of defects.

Table 2: Summarized data from PL spectra of ZnO(NRs) grown onto different substrate for 2 and 3 h.

Sample	Duration Time (h)	UV peak (nm)	Eg (ev)
Glass	2	378.8	3.27
PET	2	377.4	3.28
Si	2	377.4	3.28
Steel	2	383.3	3.23
glass	3	378.4	3.27
PET	3	379.4	3.26
Si	3	376.2	3.29
Steel	3	379.9	3.26

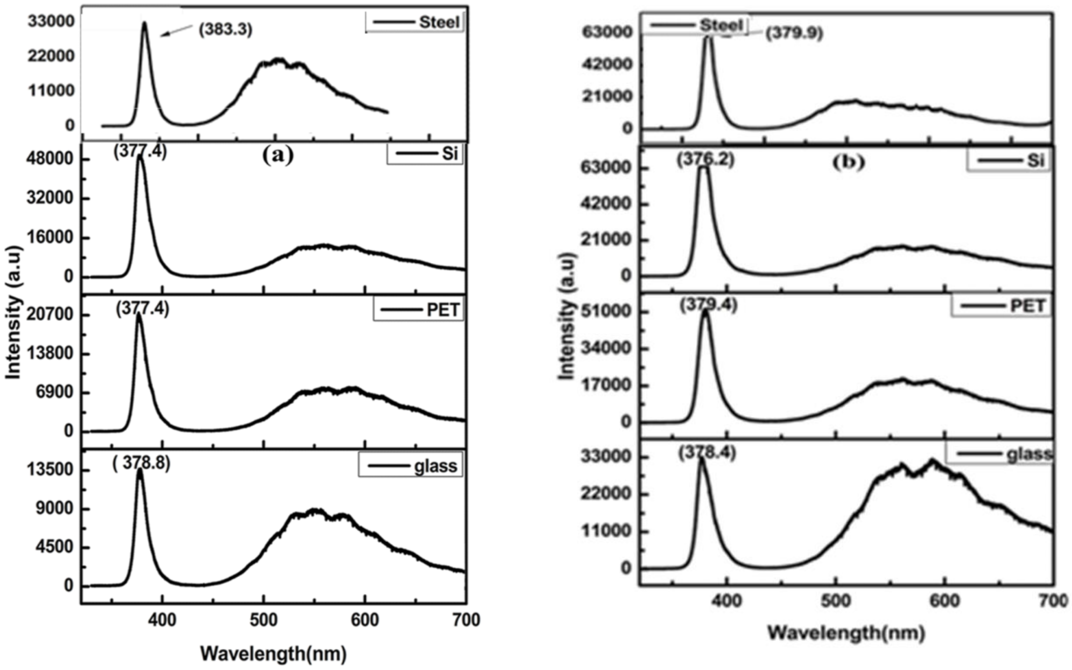

(a) (b)

Fig. 5: The PL spectra of the ZnO(NRs) at (a) 2h and (b) 3h on various substrates.

3.4 Raman Spectroscopy

It is well known that Raman spectra are sensitive to the crystal quality. Based on group theory, the Γ point of the Brillouin Zone, the existence of the following optical modes can be obtained[20, 21]:

$$\Gamma = A1 + 2B1 + E1 + 2E2 \qquad (3)$$

whereA_1, E_1 and E_2modes are Raman active while the infrared A_1 and E_1active modes split into longitudinal optical (LO) and transverse optical (TO) components [22]. Figure 6illustratesthe Raman spectra of ZnO NRs grown onto different substrates for2 and 3h. According to Raman selection rules, only modes E2 (high) and A1 (LO) [23] are allowed. The shift of E2 (high) mode gives information about the nature of stress; a compressive if E2 (high) shifts to higher values than 437 cm^{-1}, whereas a tensile stress will lead to lower values than 437 cm^{-1}[24]. It can be noticed that all films reveal a shift toward higher Raman wave number thus indicating that all grown films are under compressive stress. This result is in good agreement with XRD analysis, see Table 1. The highest value of the E2 (high) peak indicates good quality and higher crystallinity of the as-grown ZnO NRs. Finally, the remaining observed peaks originated from substrates; 521 nm from Si substrate [25], 633nm from PET substrate [26].

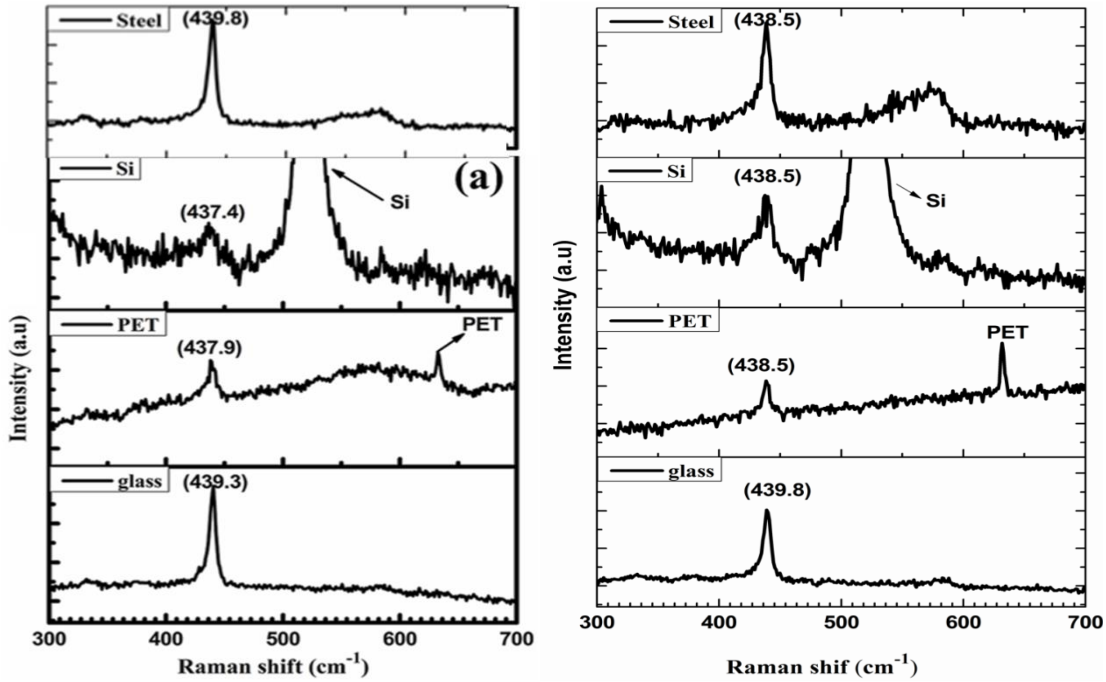

a) b)

Fig.6: Raman spectra of ZnO NRs grown onto various substratesat (a) 2h and (b) 3h.

3.5 UV Photodetector Sensitivity Measurements

The I-V characteristics of the as-fabricated photodetectors were measured before and after light exposure. Figure7 (a and b) shows the I-V curves for ZnO NRs deposited onto various substrates with (different wavelength) and without UV illumination for 2 and 3 h. It is noted that I-V curves are Schottky indicating the good Schottky contact between ZnO NRs and the Pt-electrodes. The I-V peak under UV illumination is higher than that in the dark environment. The low I-V peak is caused by the depletion layer created near the surface by adsorbed oxygen molecules in the dark environment (O_2 (gas)+e^- $O_2{}^-$]. When exposed to UV light, ZnO NRs generate e-h pair (hv e^-+h]. Then the photo-generated holes react with adsorbed oxygen molecules[h^++O_2(ad)O_2]; the trapped electrons are migrate to the conduction band to increase the carrier concentration of ZnO NRs[27, 28].The maximum response determined from Figure7 is as follow: 368 nm for glass; 368 nm for PET and 400 nm for Si and 365 nm for stainless steel. The values are very close to the value of the energy band gap of ZnO (Eg=3.37eV).

The saturation current $I_s$is given by the following expression [29, 30]:

$$I_S = A^* STexp\left(-\frac{q\Phi_\beta}{KT}\right) \qquad (4)$$

where A* is the effective Richardson constant (its theoretical value is32 A.cm^{-2}.K^{-2}); Φ_β is the Schottky barrier height; and the Schottky constant areais0.25 cm^2. From the I_s values obtained from the intercept of the linear portion of the forward I-V characteristic plots(Fig. 8a and b), the barrier height Φ_β can be calculated usingthe following equation [31]:

$$\phi_\beta = \frac{KT}{q}\ln\left(\frac{SA^*T^2}{I_S}\right) \tag{5}$$

The values of dark and light photo- saturation current I_S as well as and barrier height Φ_β before and after UV-light for the films deposited at 2 and 3 h onto (glass, PET, Si, and stainless steel) substrates are reported in Table 3.

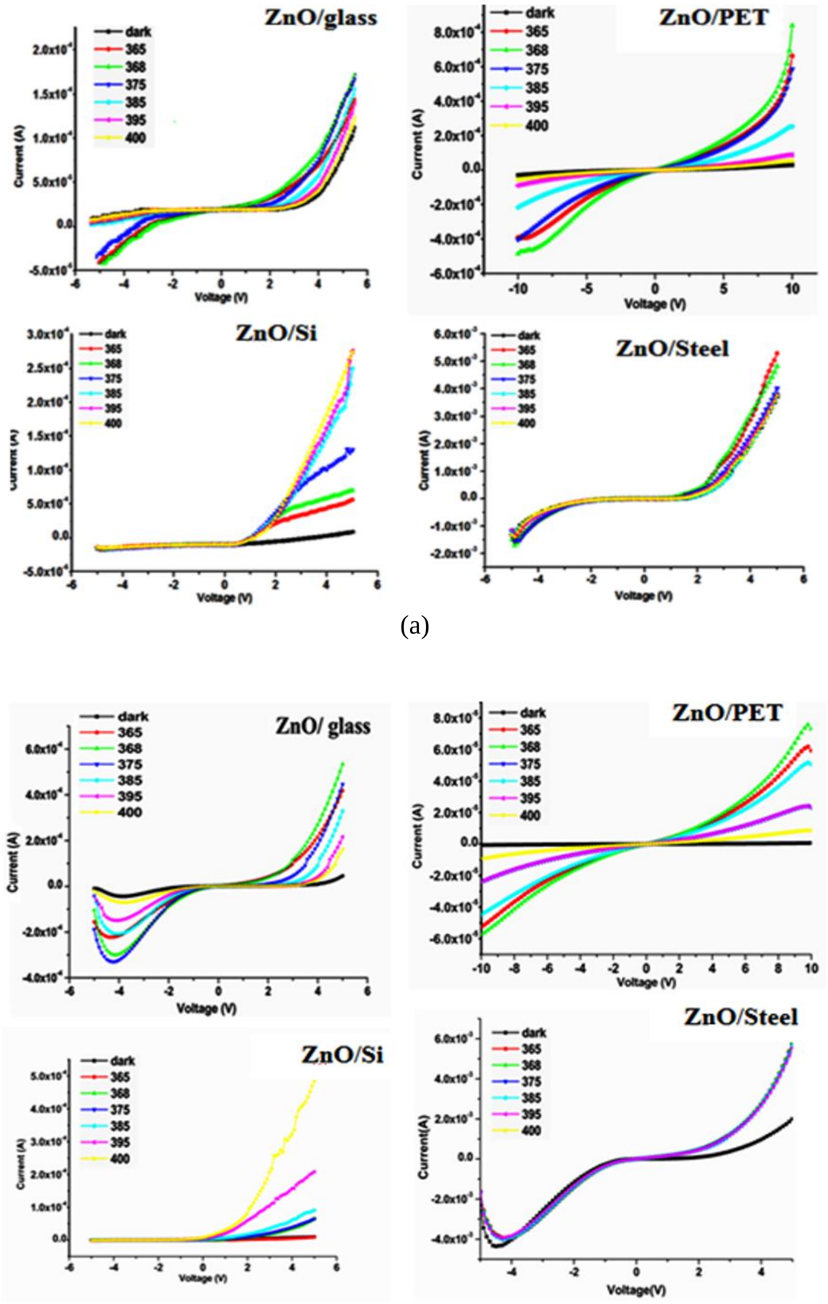

(a)

(b)

Fig. 7: I-V characteristics of Pt-ZnO(NRs)-Pt devices fabricated from ZnO NRs deposited onto various substrates at (a) 2h and (b) 3h.

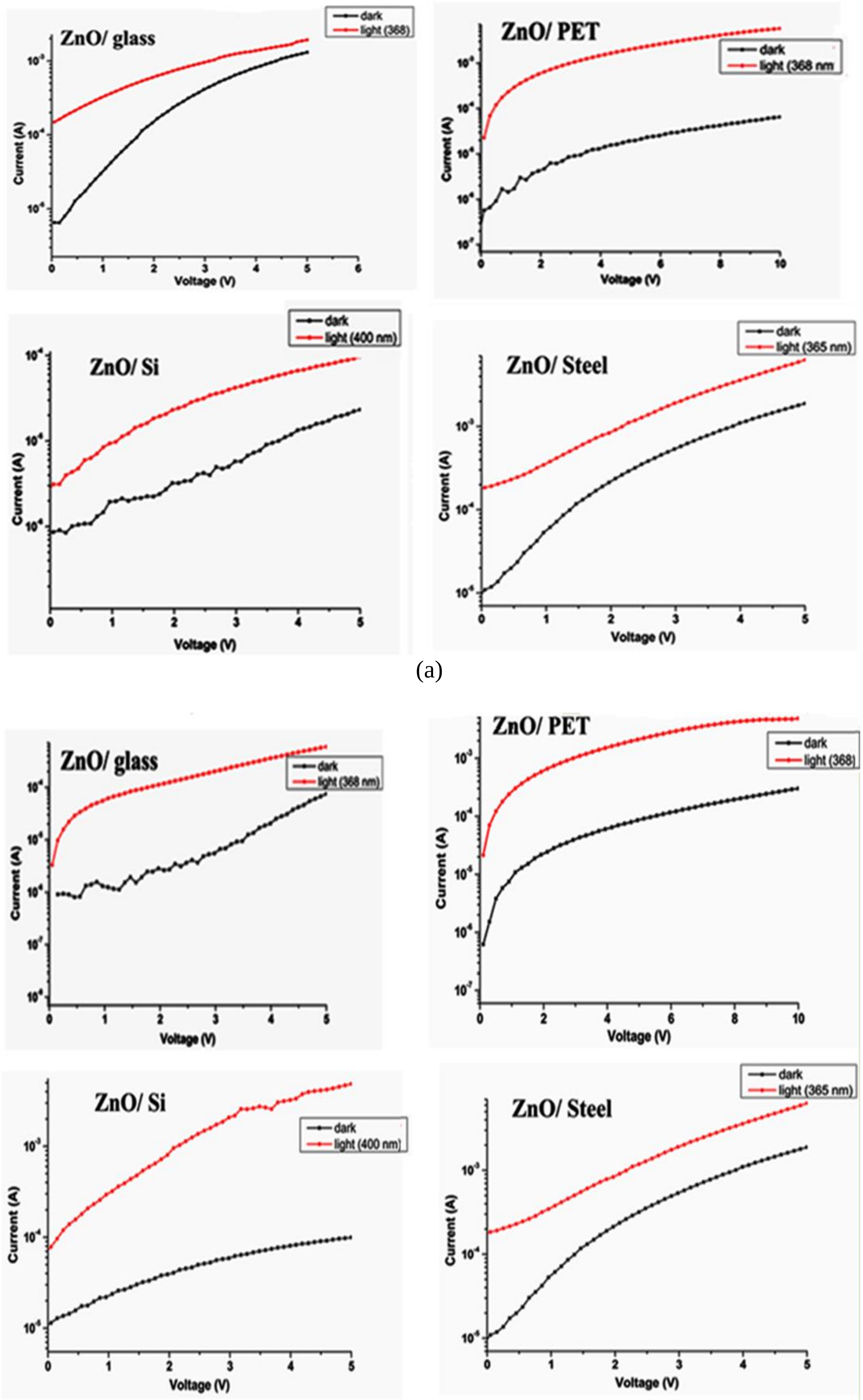

(a)

(b)

Fig. 8: Semi-logarithmic scale of the current as a function of the bias voltage (I- V) of the as deposited Schottky diodes in dark and after UV- illumination for a deposition time of(a) 2h and (b) 3h.

Table 3: Schottky diode parameters at 5V for dark and under light of ZnO NRs grown onto different substrate for 2 and 3 h.

Sample	**In dark**			**In light**		
Deposited time/ substrate	I_d (A)	I_S (A)	Φ_β (eV)	I_{Ph} (A)	I_S (A)	Φ_β (eV)
2h / Glass	$1.20*10^{-4}$	$5.5*10^{-6}$	0.697	$1.80*10^{-4}$	$1*10^{-4}$	0.622
2h / PET	$0.2*10^{-5}$	$4*10^{-7}$	0.764	$8.2*10^{-4}$	$2*10^{-5}$	0.663
2h / Si	$2.5*10^{-5}$	$8.5*10^{-7}$	0.745	$2.85*10^{-4}$	$4*10^{-6}$	0.705
2h / Stainless steel	$3.89*10^{-3}$	$0.2*10^{-6}$	0.691	$6.50*10^{-3}$	$7*10^{-6}$	0.663
3h / Glass	$7.48*10^{-5}$	$1*10^{-4}$	0.622	$5.93*10^{-4}$	$4*10^{-4}$	0.586
3h / PET	$0.2*10^{-5}$	$5*10^{-7}$	0.759	$2.5*10^{-5}$	$2*10^{-5}$	0.663
3h / Si	$2.32*10^{-5}$	$0.2*10^{-5}$	0.713	$4.70*10^{-4}$	$7*10^{-5}$	0.631
3h / Stainless steel	$1.99*10^{-3}$	$1*10^{-5}$	0.681	$5.81*10^{-3}$	$1.8*10^{-4}$	0.607

The obtained current for all substrates was higher than the dark current over the entire range of the applied voltage. The as-obtained high photocurrent can be related to the obtained decrease in Shottky barrier heights (Φ_β) under UV light. The barrier height value of ZnO (NRs) grown at 3h was less than that at 2h, which revealed that the growth of ZnO(NRs) at 3h represented the best quality. This result is in good agreement with FESEM and X-ray results. Figure 9 (a and b) shows the switch on- off characteristic of MSM based ZnO(NRs) at different bias voltages (1, 3 and 5 V). Illumination was switched on and off periodically at a regular period of time of 20 s. From the results reported in Table 4, it can be noticed that the current increases when the photodetector device was illuminated then decreases when the light was switched off. When the device is illuminated with energy equal or more than the energy gap of material, electron – hole pairs will be created by optical absorption.

The rise time was defined as the time needed to reach 90% of the photocurrent from dark current value after light exposure whereas the decay time is defined as the time needed to reach 10% of the photocurrent after switching off the light exposure. The high sensitivity, gain and faster response times were observed for ZnO NRs deposited for 2 and 3h onto Si substrate by 400nm light, due to the enhanced crystallinity for3h, which implies a very low defects density and high density of deposited ZnO NRs, thus, rapid saturation and decay of the photocurrent. Once again, this is in good agreement with FESEM, XRD and Raman results.

The sensitivity of the as-fabricated devices was determined at different applied bias voltage using the equation [32]:

$$S = \frac{I_{ph} - I_{dark}}{I_{dark}} \times 100 \qquad (6)$$

whereI_{ph} and I_{dark} are the photocurrent and dark current, respectively.

It is found that for ZnO NRs deposited onto stainless steel substrate, the measurement of pulse photo-response was not possible because of the high short circuit between the top contact (ZnO) and the substrate (stainless steel). Table 4 summarizes the electrical properties of various ZnOnanorods-based UV photodetectors. The fast photoresponse and high gain of the UV photodetectors based on ZnO(NRs) grown at 3h compared with values obtained at 2h, and the fast photoresponse and high gain ZnO(NRs)/Si compared with other substrates, confirmed that of ZnO(NRs) grown by CBD method at 3h onto Si substrate possessed an enhanced crystallinity and large photoactive surface area. Due to the high sensitivity of ZnO(NRs)/Si photodetector at 1V, we measured pulse UV detector at zero voltage, seeFigure10. We can notice a very high sensitivity; approximately 6250. In the dark, The Schottky barrier height is formed at the Pt–ZnO interfaces, where the Pt electrode and ZnO have the same Fermi energy level. According to the theory. Under UV illumination, electron–hole pairs are generated in ZnO. The generated electrons in the conduction band (CB) tend to move away from the contact, while the holes in the valence band (VB) tend to move close to the interface toward the metal side. So that the effective height of the Schottky barriers is lowered, resulting in an increase in free carrier density and thus the obtained photocurrent [33, 34]

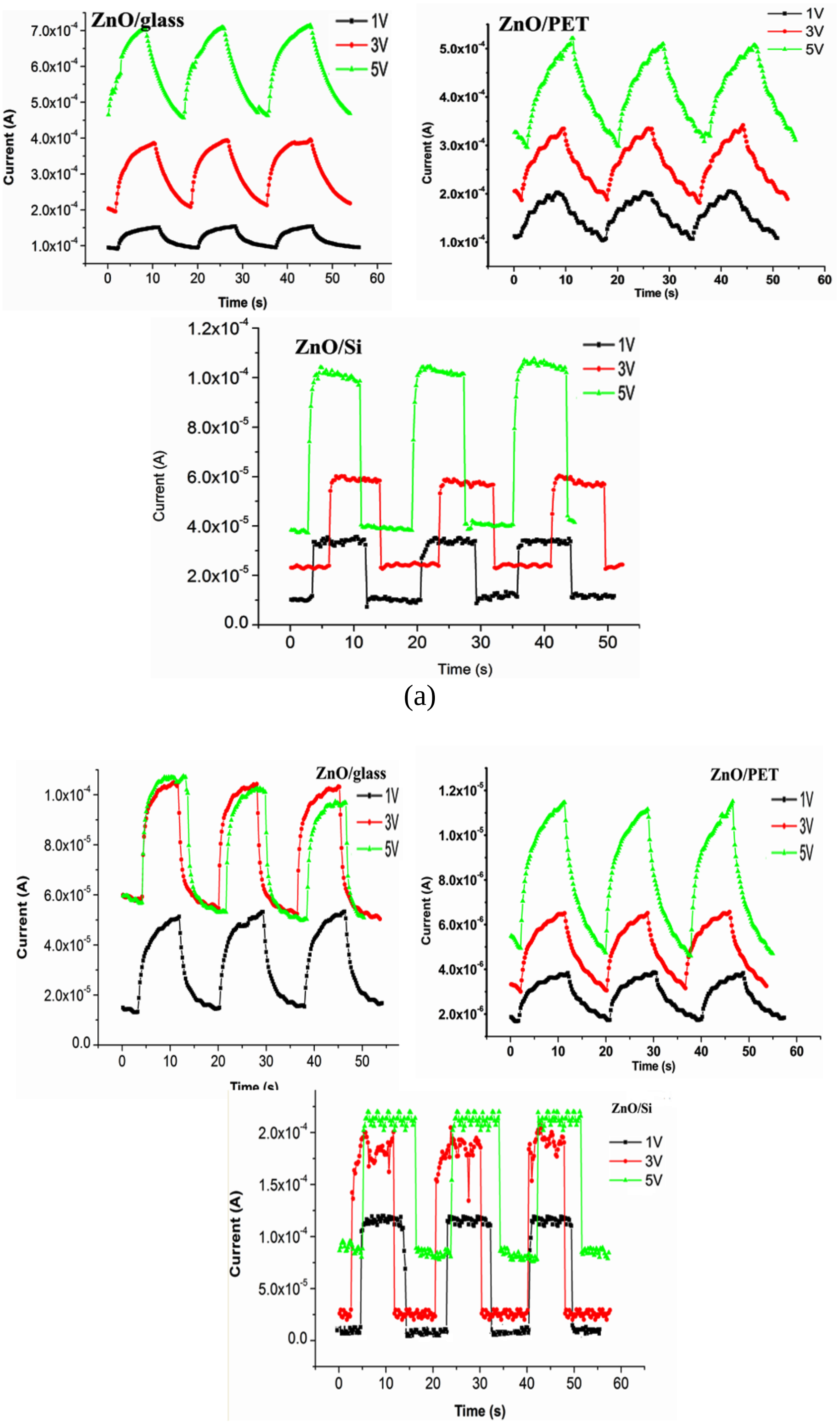

(a)

(b)

Fig.9: UV ON/OFF photo –response of ZnO(NRs) arrays grown onto various substrates for(a) 2h and (b) 3h.

The high sensitivity and faster response at zero bias voltage of the as-fabricated photodetector make this device a promising and potential self-powered UV detector. The most interesting properties of our UV photodetector consist on its ultra-fast response and recovery times at zero bias voltage. The response and recovery times for this UV photodetectorare equal to 0.864s and 0.875s, respectively. The faster response and recovery times confirmed that ZnO (NRs) possess high structural quality with less defects. On the other side, only few studies have reported on UV detectors fabricated with zero bias voltage [35-37].

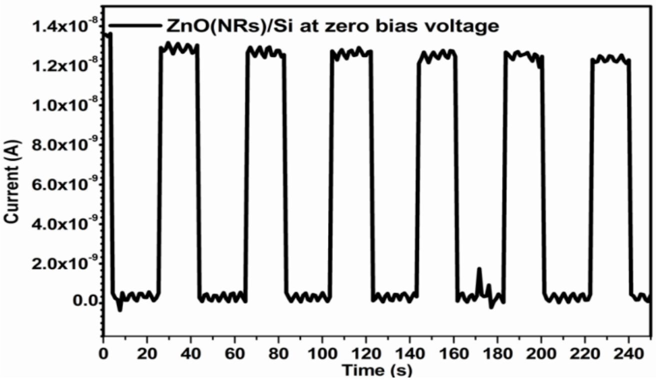

Fig. 10: The repeatability property (ON/OFF) of UV detector based on ZnO (NRs) arrays deposited onto Si substrate for 3h upon exposure to 400 nm light at zero bias voltage.

Table 4: The response and recovery times, gain and sensitivity of UV detector under different bias voltages grown onto different substrate for 2 and 3 h.

Substrate/ Deposited Time	BiasVoltage(V)	Response Time(s)	Recovery Time (s)	Sensitivity (%)	Gain
Glass/ 2H	1 3 5	5.1 5.0 4.0	3.3 3.0 3.7	57.8 94 56.5	1.45
Si/ 2H	1 3 5	0.3 0.3 0.5	0.1 0.1 0.1	220 163 184	28
PET/ 2H	1 3 5	4.8 4.8 4.2	4.4 3.5 5.2	63 94.4 71	9
Steel / 2H	1 3 5	-------------	---- ----- ----	------ ---- ----	1.67
Glass/ 3H	1 3 5	5.1 3.2 3.6	4.9 3.9 4.8	257 86 76	7.92
Si / 3H	1 3 5	0.1 0.1 0.1	0.1 0.1 0.1	1000 620 200	50
PET / 3H	1 3 5	3.6 2.8 3.9	5.8 5.5 5.1	121 113 132	14
Steel / 3H	1 3 5	---------------	-------------	-------------	2.91

4. Conclusion

Nanostructured ZnO photodetector has been successfully synthesized onto glass, PET, n-type Si, and stainless steel substrates with an inter digital Pt comb-like electrode using chemical bath deposition. XRD analysis and FESEM observations indicate the growth of high density arrays of hexagonal wurtzite ZnO nanorods in a predominantly (002) orientation. Raman spectra showed that all films reveal a shift toward higher 437 cm^{-1}, indicating that all films are subjected to compressive stress. The I-V curves recorded for the UV detector indicate that the current increases when exposed under UV visible and higher sensitivity for ZnO(NRs)grown onto Si substrate; 6250 at zero bias voltage. This means that the as-fabricated ZnO (NRs)/Si UV detector can work as self-powered device.

Acknowledgments

The authors would like to thank the Nano-Optoelectronics Research and Technology Laboratory (N-O-R) of the School of Physics , University Sains Malaysia.

References

[1] O. Lupan, V. Ursaki, G. Chai, L. Chow, G. Emelchenko, I. Tiginyanu, A. Gruzintsev, A. Redkin, Sensors and Actuators B: Chemical, **144**,56 (2010).

[2] J. Hassan, M. Mahdi, C. Chin, H. Abu-Hassan, Z. Hassan, Sensors and Actuators B: Chemical, **176**,360 (2013).

[3] O. Lupan, V. Guérin, I. Tiginyanu, V. Ursaki, L. Chow, H. Heinrich, T. Pauporté, Journal of Photochemistry and Photobiology A: Chemistry, **211**,65 (2010).

[4] O. Lupan, V. Guérin, L. Ghimpu, I. Tiginyanu, T. Pauporté, Chemical Physics Letters, **550,**125 (2012).

[5] J. Hassan, M. Mahdi, Y. Yusof, H. Abu-Hassan, Z. Hassan, H. Al-Attar, A. Monkman, Optical Materials, **35,**1035 (2013).

[6] O.F. Farhat, M.M. Halim, M.J. Abdullah, M.K. Ali, N.K. Allam, Beilstein journal of nanotechnology, **6,**720 (2015).

[7] S.M. Mohammad, Z. Hassan, N.M. Ahmed, N. Al-Hardan, M. Bououdina, Journal of Materials Science: Materials in Electronics, **26**,1322 (2015).

[8] X. Su, Z. Zhang, M. Zhu, Applied physics letters, **88**,61913 (2006).

[9] Ü. Özgür, Y.I. Alivov, C. Liu, A. Teke, M. Reshchikov, S. Doğan, V. Avrutin, S.-J. Cho, H. Morkoc, Journal of applied physics, **98**,041301 (2005).

[10] K. Liu, M. Sakurai, M. Aono, ZnO-based ultraviolet photodetectors, Sensors**10**,8604 (2010).

[11] B. Mullins, S. Soares, K. McArdle, C. Wilson, S. Brueck, Photonics Technology Letters, IEEE, **3**,360 (1991).

[12] A. Uzum, T. Ashikaga, T. Noguchi, H. Kanda, T. Matsuoka, T. Nakanishi, H. Fukui, T. Harada, S. Ito, International Journal of Photoenergy, 2015 (2015).

[13] J. Hassan, Z. Hassan, H. Abu-Hassan, Journal of Alloys and Compounds, **509**,6711 (2011).

[14] N.S. Ridhuan, K.A. Razak, Z. Lockman, A.A. Aziz, Structural and morphology of ZnO nanorods synthesized using ZnO seeded growth hydrothermal method and its properties as UV sensing, (2012).

[15] P. Kumbhakar, D. Singh, C. Tiwary, A. Mitra, CChalcogenide letters, **5,**387 (2008).

[16] K. Kamarudin, S.M. Mamduh, A.Y. Md Shakaff, S. Mad Saad, A. Zakaria, A.H. Abdullah, L.M. Kamarudin, Instrumentation Science & Technology, **43,**74 (2015).

[17] O. Farhat, M. Halim, M. Abdullah, M. Ali, N.M. Ahmed, N.K. Allam, Applied Physics A, **119**,1197 (2015).

[18] A. Umar, S. Kim, Y. Hahn, Superlattices and Microstructures, **39,**145 (2006).

[19] G. Kenanakis, M. Androulidaki, E. Koudoumas, C. Savvakis, N. Katsarakis, Superlattices and Microstructures, **42**,473 (2007).

[20] J. Zhao, X. Yan, Y. Yang, Y. Huang, Y. Zhang, Materials Letters, **64**,569 (2010).

[21] F. Tong, K. Kim, Y. Wang, R. Thapa, Y. Sharma, A. Modic, A. Claude Ahyi, T. Issacs-Smith, J. Williams, H. Ahn, Growth of ZnO nanorod arrays on flexible substrates: effect of precursor solution concentration, ISRN Nanomaterials, 2012 (2012).

[22] F. Decremps, J. Pellicer-Porres, A.M. Saitta, J.-C. Chervin, A. Polian, Physical Review B, **65**,092101 (2002).

[23] R. Wang, G. Xu, P. Jin, Physical Review B, **69**,113303 (2004).

[24] N. Hassan, M. Hashim, M. Bououdina, Ceramics International, **39,**7439 (2013).

[25] C. Droz, E. Vallat-Sauvain, J. Bailat, L. Feitknecht, J. Meier, A. Shah, Solar Energy Materials and Solar Cells, **81,**61 (2004).

[26] J. Purvis, D. Bower, Journal of Polymer Science: Polymer Physics Edition, **14**,1461 (1976).

[27] S. Panda, C. Jacob, Solid-State Electronics, **73**,44 (2012).

[28] M. Rajabi, R. Dariani, A.I. Zad, Sensors and Actuators A: Physical, **180,**11 (2012).

[29] C. Singh, G. Agarwal, G.D. Rao, S. Chaudhary, R. Singh, Materials Science in Semiconductor Processing, **14**,1 (2011).

[30] F. Hossein-Babaei, S. Abbaszadeh, M.S. Esfahani, Fabrication and assessment of a gas sensitive silver-rutile Schottky diode.

[31] W. Mtangi, F.D. Auret, C. Nyamhere, P.J. van Rensburg, A. Chawanda, M. Diale, J.M. Nel, W.E. Meyer, Physica B: Condensed Matter, **404,**4402 (2009).

[32] B. Yuan, X.J. Zheng, Y.Q. Chen, B. Yang, T. Zhang, Solid-State Electronics, **55,**49 (2011).

[33] H.-Y. Chen, K.-W. Liu, X. Chen, Z.-Z. Zhang, M.-M. Fan, M.-M. Jiang, X.-H. Xie H.-F. Zhao, D.-Z. Shen, Journal of Materials Chemistry C, **2,**9689 (2014).

[34] Y. Hu, J. Zhou, P.H. Yeh, Z. Li, T.Y. Wei, Z.L. Wang, Advanced Materials, **22,**3327 (2010).

[35] H. Zhou, P. Gui, Q. Yu, J. Mei, H. Wang, G. Fang, Journal of Materials Chemistry C, **3**,990 (2015).

[36] Z. Bai, X. Yan, X. Chen, Y. Cui, P. Lin, Y. Shen, Y. Zhang, RSC Advances, **3,**17682 (2013).

[37] X. Zhao, R. Zhou, Q. Hua, L. Dong, R. Yu, C. Pan, Journal of Nanomaterials, 2015 (2015).